Journal of
Composites Science

MDPI

Article

White Ginger Nanocellulose as Effective Reinforcement and Antimicrobial Polyvinyl Alcohol/ZnO Hybrid Biocomposite Films Additive for Food Packaging Applications

Dieter Rahmadiawan [1], Hairul Abral [2,3,*], Wahyu Hidayat Yesa [2], Dian Handayani [4], Neny Sandrawati [4], Eni Sugiarti [5], Ahmad Novi Muslimin [5], S. M. Sapuan [6] and R. A. Ilyas [7]

1 Department of Mechanical Engineering, Faculty of Engineering, Universitas Negeri Padang, Padang 25171, Indonesia
2 Laboratory of Nanoscience and Technology, Department of Mechanical Engineering, Andalas University, Padang 25163, Indonesia
3 Research Collaboration Center for Nanocellulose, BRIN-Andalas University-Institut Teknologi Batam (ITEBA, Batam), Padang 25163, Indonesia
4 Laboratory of Sumatran Biota, Faculty of Pharmacy Andalas University, Padang 25163, Indonesia
5 Laboratory of High Resistance Materials, Research Center for Physics, Indonesian Institute of Sciences (LIPI), Tangerang Selatan 15310, Indonesia
6 Department of Mechanical and Manufacturing Engineering, Faculty of Engineering, Universiti Putra Malaysia (UPM), Serdang 43400, Malaysia
7 School of Chemical and Energy Engineering, Faculty of Engineering, Universiti Teknologi Malaysia, Johor Bahru 81310, Malaysia
* Correspondence: abral@ft.unand.ac.id

Abstract: Polyvinyl alcohol (PVA) has been used in packaging applications due to its biocompatibility and biodegradability. However, this non-toxic synthetic material belonging to a highly hydrophilic polymer has poor resistance to wet environments, no antibacterial activity, and low tensile and thermal properties. This study aims to prepare and characterize a PVA-based biocomposite film mixed with antimicrobial white ginger nanocellulose (GCNF) and zinc oxide (ZnO) nanoparticles. The film was processed using GCNF (0.1 g) or/and ZnO nanoparticles (0.5 g). The results confirm that the GCNF/ZnO/PVA-based film presents the strongest antimicrobial activity and the highest thermal resistance. This film also had the best value in tensile strength (19.7 MPa) and modulus (253.1 MPa); 63.9% and 117.9%, respectively higher than purce PVA. Its elongation at break was 56.6%, not statistically significantly different from the pure PVA film. Thus, this PVA-based hybrid biocomposite film reinforced by GCNF and ZnO has excellent potential for fresh food packaging in industrial applications.

Keywords: white ginger; Polyvinyl alcohol; zinc oxide; biocomposite; biofilm

Citation: Rahmadiawan, D.; Abral, H.; Yesa, W.H.; Handayani, D.; Sandrawati, N.; Sugiarti, E.; Muslimin, A.N.; Sapuan, S.M.; Ilyas, R.A. White Ginger Nanocellulose as Effective Reinforcement and Antimicrobial Polyvinyl Alcohol/ZnO Hybrid Biocomposite Films Additive for Food Packaging Applications. *J. Compos. Sci.* **2022**, *6*, 316. https://doi.org/10.3390/jcs6100316

Academic Editors: Francesco Tornabene and Thanasis Triantafillou

Received: 18 September 2022
Accepted: 13 October 2022
Published: 17 October 2022

1. Introduction

Recently, composite materials is preferable in many aspect [1–3]. It can be applied in food packaging, which protects foods against deterioration because of microorganisms, odors, and dust [4]. The most commonly used food packaging materials include petroleum products [5]. The widespread use of this material leads to severe problems for environmental impact because of poor biodegradability [6]. PVA has been used in food packaging applications due to its biocompatibility and biodegradability [7]. However, this non-toxic synthetic material belonging to a highly hydrophilic polymer has poor resistance to wet environments [8]. PVA also presents no antibacterial activity and has low tensile and thermal properties [9]. Many efforts have been conducted to minimize these weaknesses by mixing PVA with fillers [10].

The nanocellulose used as reinforcement in these films lacks antimicrobial activity. Some previous works have added zinc oxide (ZnO) nanoparticles to produce antibacterial

PVA/cellulose-based biocomposite films [11]. It also provide corrosion resistance, and strong mechanical properties [12,13]. However, ZnO, which is much more expensive than natural fibers, increases the production cost of a PVA/ZnO/cellulose biocomposite film [14]. An antimicrobial nanocellulose can be obtained from white ginger tubers [15]. This plant is abundantly available in tropical countries like Indonesia, one of the five largest producers of ginger for the global market (228,707 metric tons in 2019) [16]. Ginger oil and oleoresin are extracted from the tuber, leaving a large residual of discarded biomass [17]. Recently, we successfully prepared a highly transparent cellulose film with good antimicrobial activity from this source [18]. After adding ginger cellulose, the tensile strength improved by 65% compared to pure PVA, and it also has high thermal resistance up to 350 °C [19]. Thus, it could be expected that the addition of ginger nanocellulose along with ZnO nanoparticles would produce a cheap PVA biocomposite film with strong mechanical properties, and higher antimicrobial properties [20].

Numerous nanocellulose-based materials have been advanced for various applications [21–24]. However, the properties of an environmentally friendly film that consists of PVA, ZnO, and white ginger nanocellulose (GCNF) have not yet been explored. Introducing the GCNF into the biocomposite film would reduce the usage of inorganic ZnO, making the product cheaper and more environmentally friendly. Therefore, this present study produced and compared the properties of pure PVA and PVA-based biocomposite films mixed with white ginger nanofiber or/and ZnO nanoparticles. Effects of these nanofillers on tensile and thermal properties, resistance, and antimicrobial activity of the sample were investigated.

2. Materials and Methods

2.1. Materials

The GCNF was prepared using residue fibers isolated from white ginger (Zingiber officinale var. Roscoe) roots from a local market, Padang, Indonesia. Isolation of the GCNF was carried out using reagents including CH3COOH (density 1 g/cm^3), toluene (99%), NaClO2 80% (Sigma-Aldrich, Singapore), distilled water, ethanol 96% (Andeska Laboratory, Padang, India), NaOH (Brataco, Padang, India), and HCL 37% (Merck KGaA, Darmstadt, Germany). PVA powder (average molecular weight of 0.9 × 105 g/mol and a minimum degree of hydrolysis of 87%) was bought from PT. Brataco, Padang, Indonesia.

2.2. Preparation of Nanocellulose and Hybrid Biocomposite Films

The detail of the preparation method, including the GCNF morphology, and the crystallinity index used in this work, are available in our previous work [18]. The residue ginger fibers were immersed in a solution (ethanol and toluene with a ratio of 1:2). Next, the solution was heated using a Daihan Scientific MSH-200 magnetic stirrer at 50 °C, 500 rpm for 48 h. The fibers were rinsed and screened through a filter (200T mesh) with distilled water until pH 7. The wet fiber was dried with a drying apparatus (Oven Memmert UN-55) at 50 °C for 20 h, then was treated with a 5% NaOH, and heated at 500 rpm, 50 °C for 4 h in the stirrer. The suspension after neutralization (pH 7) with distilled water was screened with a filter (200T mesh). Then the wet fibers were dried in a drying cabinet at 50 °C for 20 h. These dry fibers were ground and chopped with an electric mixer. Then they were soaked with a mixture of CH_3COOH and $NaClO_2$ (a ratio of 1:4). Next, the mixture was heated at 60 °C for 2 h, 500 rpm, with the hot stirrer. Then it was rinsed until it is neutral. Next, a hydrolysis process using 5M HCl at 50 °C was conducted. This fiber (200 mL) was treated with an ultrasonic probe sonicator (600 W, below 60 °C). The suspension was heated at 50 °C for 20 h in the drying oven. The preparation of the PVA-based biocomposite film was relatively similar to our previous work [19]. Table 1 displays the ratios of nanofillers (GCNF and ZnO), PVA powder, and distilled water used in the studied films. The total weight for each film was 100 g. The solution for each sample was heated by a Daihan MS-H280-Pro. Next, the biocomposite gel was dried in a vacuum oven (0.6 MPa, 50 °C, 21 h). Then, all dried samples were stored in a closed desiccator (50% RH, 25 °C). Labeling of the films was shown in Table 1.

Table 1. The ratio of PVA powders, nanofillers (GCNF and ZnO nanoparticles), and distilled water.

Samples	PVA (g)	Distilled Water (mL)	GCNF (g)	ZnO (g)
PVA	10	90	-	-
PVA/ZnO	10	89.5	-	0.5
PVA/GCNF	10	65.7	24.3 or 0.1	-
PVA/ZnO/GCNF	10	65.2	24.3 or 0.1	0.5

2.3. Sample's Morphology Using SEM

The surface morphology of the sample's fracture was observed using a SEM (JFIB 4610, Tokyo, Japan). All specimens were coated with gold for 1 min to enhance the conductivity. An accelerating voltage was regulated during testing. The detailed of this test is similar to our prior published work [20]

2.4. Tensile Test

The standard method ASTM D638- type V was used for tensile testing (ASTM D638-V 2012). Tensile strength (TS), tensile modulus (TM), and elongation at break (EB) of the sample were measured using a Com-Ten testing machine 95T. All samples before testing were stored in a closed desiccator (50% RH, 25 °C) for 48 h. Tensile tests were repeated five times for each film.

2.5. Fourier-Transform Infrared (FTIR) Spectroscopy

FTIR measurement of the functional groups of the films was carried out using PerkinElmer equipment (PerkinElmer, Waltham, MA, USA).

2.6. X-ray Diffraction (XRD)

The X-ray diffraction testing was conducted using PANalytical Xpert PRO (Philips Analytical, Almelo, The Netherlands). The Cu-Kα radiation source (λ = 0.1542 nm) was applied. Specimens with a diameter of 10 mm were stored in a closed chamber (50% RH at 25 °C) for 48 h. It was placed on a specimen holder. The samples were scanned with a scan step of 0.02 degree/s from 2θ = 10° to 50° [25].

2.7. Thermogravimetric Analysis (TGA)

A thermal resistance instrument (DTG-60, Shimadzu) was used to measure the sample's TGA and DTG. A nitrogen flow rate of 50 mL/min and a heating rate of 10 °C/min were used during testing the sample.

2.8. Antimicrobial Activity

Antimicrobial activity tests for each sample were carried out against *Staphylococcus aureus* (SA), *Bacillus substilis* (BC), *Escherichia coli* (EC), *Pseudomonas aeruginosa* (PA), and *Candida albicans* (CA) using the agar diffusion method [26]. The bacteria and fungi were grown in nutrient agar (NA) and Sabouraud dextrose agar (SDA), respectively. The film samples were prepared with a diameter of 6 mm, and put on the NA and SDA medium, respectively. As positive controls, disks containing chloramphenicol and nystatin (Oxoid®) in a concentration of 100 unit/disk (antifungal) were used. The antimicrobial effect was assessed by measuring the diameter of the clear zone around the films after 24 h incubation at 25–27 °C for fungi and at 37 °C for bacteria. Each test was done in triplicate.

3. Results and Discussions

3.1. FESEM Images of the Fractured Surface

The FESEM morphology of the fracture surfaces generated from the tensile tests on all samples is shown in Figure 1. Pure PVA film presents the smooth fracture surface (Figure 1a). This result indicates relatively unobstructed crack propagation passing through

this film. The addition of the nanofiller, whether ZnO or GCNF, into the PVA matrix led to a rougher fracture surface (Figure 1b). No filler agglomeration was seen owing to the excellent mixing and dispersion from ultrasonication. The nano-sized fillers were evenly dispersed in the matrix (white arrow). The fillers were firmly embedded in the PVA matrix. Consequently, fracture paths take longer tortuous pathways via the weaker parts of the sample. Due to the higher filler loadings, obstructions to this path yield more sections with beach marks (brown arrow) on the fracture surface [19]. As shown in Figure 1c, the nanofibers formed embedded loops in the PVA matrix (red arrow) which anchored the polymer chains of PVA against the movement. This result demonstrates effective interfacial adhesion between PVA and fillers due to the covalent crosslinking. The fracture surface of the hybrid biocomposite film exhibits beach marks evenly distributed over the entire surface, clarifying good nanofiller (ZnO and GCNF) dispersion.

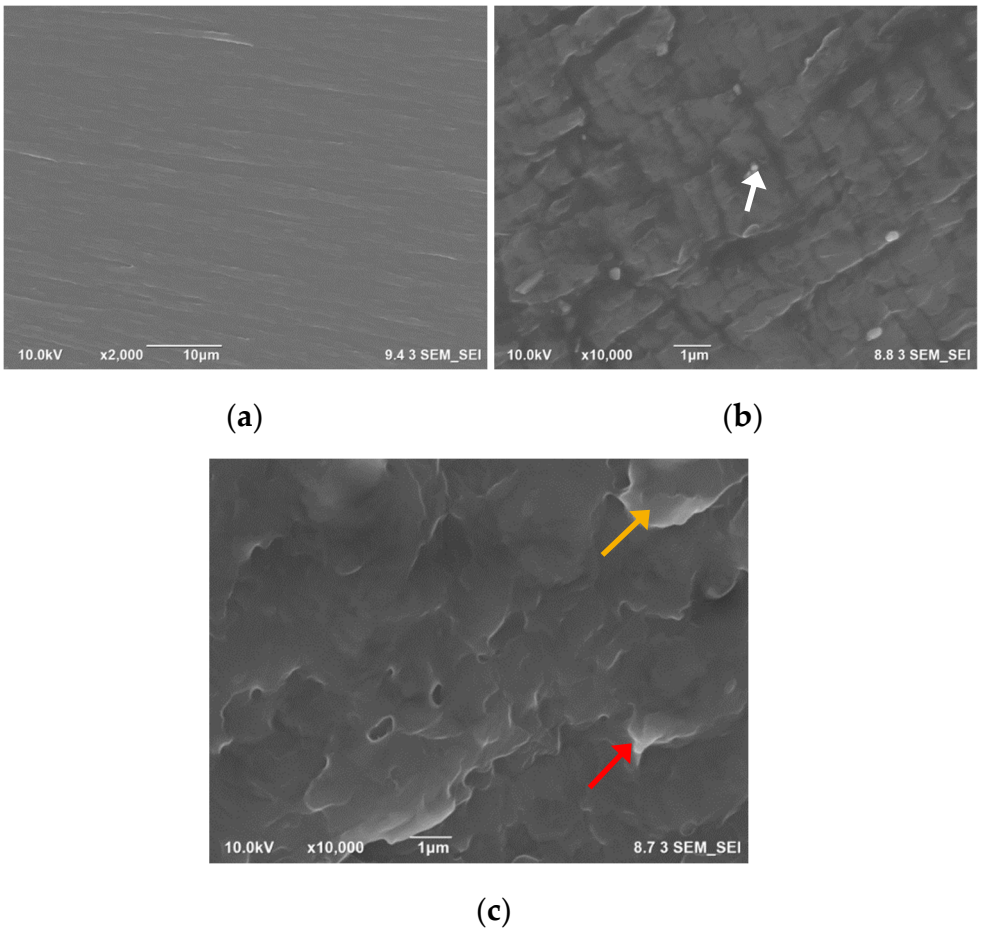

Figure 1. FESEM morphology of the fracture surface of tensile samples: (**a**) the smooth surface of pure PVA, (**b**) good dispersion of individual filler (white arrow), and (**c**) a looped filler (red arrow) and a beach mark (brown arrow) on the PVA/ZnO/GCNF biocomposite film surface.

3.2. FTIR Spectra

Figure 2a displays FTIR spectra showing all the characteristic peaks of pure PVA and biocomposites with nanofillers ZnO or/and GCNF. Bands at about 3300, 2926, 1721, 1564, and 1082 cm^{-1} attributed to O-H stretching, C-H stretching, C-O stretching, N-H bending, and C-O stretching vibrations, respectively [27,28]. All the samples display similar patterns confirming that fillers did not alter the functional groups of the PVA. However, different filler loadings did lead to changes in intensity (transmittance value), wavenumber, and some peak shapes. For example, these changes are observed on the band of about 3300 cm^{-1}, which is correspond to O-H stretching vibration (Figure 2b).

The wavenumber of the O-H stretching shifts to higher values with increasing the filler loadings (Figure 2b). This finding corresponds to an increase in hydrogen bonds from PVA and the nanofillers [29]. Furthermore, the weaker peak intensity indicated a reduction in the number of free O-H groups leading to a more hydrophobic biocomposite [30]. The weakest intensity was observed in the PVA/ZnO/GCNF-based film, attributable to the lowest number of the free hydroxyl groups and the lowest degree of hydrophilicity [31]. Some previous work proved that ZnO could decrease the hydrophilicity of PVA. The water contact angle is increased up to 79° compared with the pure PVA, which is enhanced by 125% [32]. The wavenumbers of peaks at around 1570 cm^{-1} (N-H bending) (Figure 2c) and 1082 cm^{-1} (C-O stretching) (Figure 2d) also changed with the addition of filler into the matrix due to the formation of hydrogen bonds between these functional groups on the PVA polymer and ZnO or/and GCNF [29].

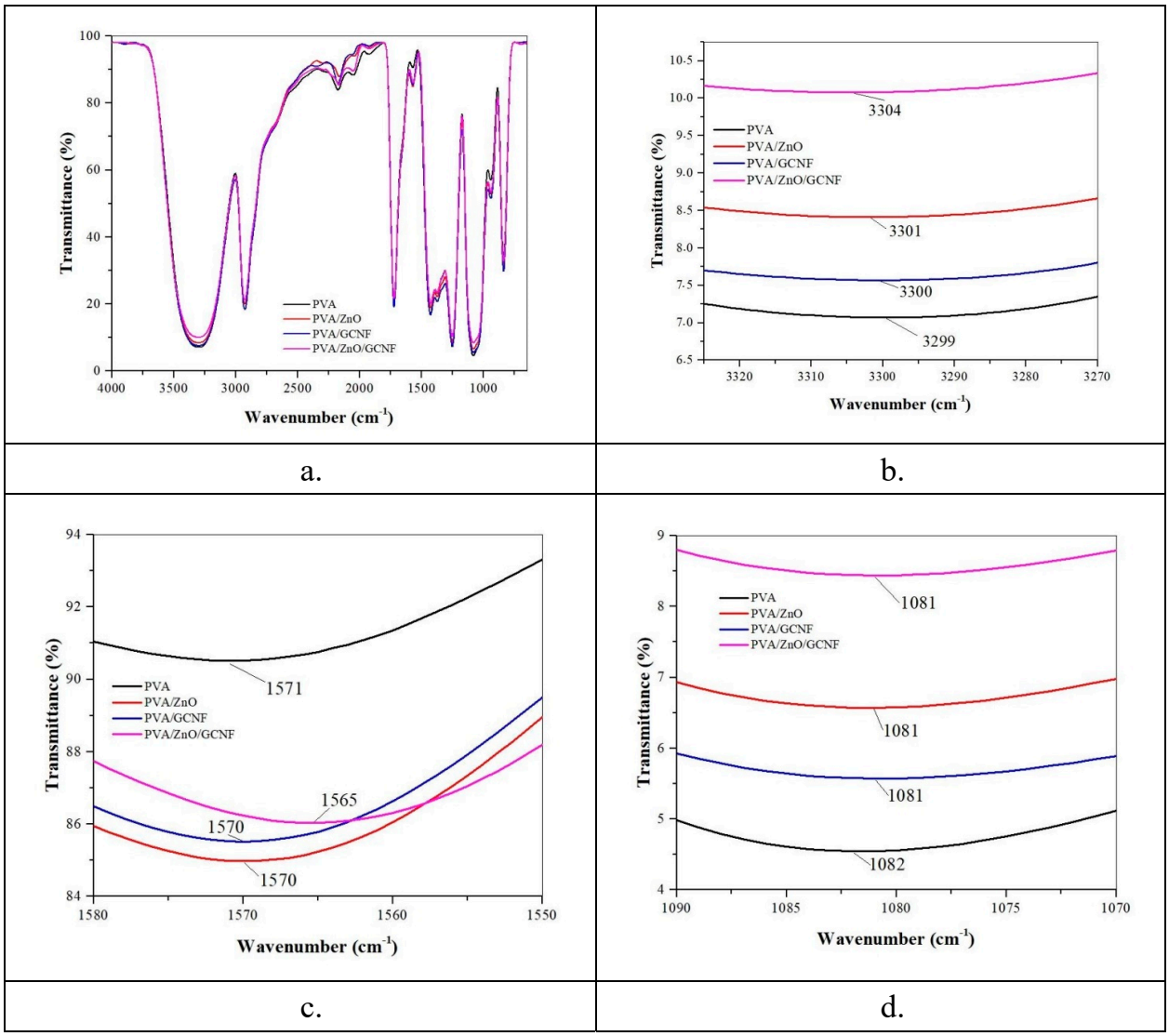

Figure 2. (**a**) FTIR spectra for all the characteristic peaks of pure PVA and the biocomposite films, (**b**) O-H stretching band, (**c**) N-H bending band, and (**d**) C-O stretching vibrations band.

3.3. X-ray Diffraction

Figure 3 displays X-ray diffraction patterns for all samples. Pure PVA film had crystalline diffraction peaks at 2θ = 12.2° and 19.6°, which correspond to the (−110) and (110) crystal planes [33]. The characteristic set of three main peaks for ZnO nanoparticles was observed in the 2θ range of 31.8, 34.4, and 37.3° corresponding to crystal planes

of (1 0 0), (0 0 2), and (1 0 1), respectively [34]. All the diffraction peaks at 2θ around 19.6° after adding the filler shifted to lower 2θ values due to an increased crystal plane spacing [31]. As presented in Table 2, *d*-spacing at 2θ around 19.6° of pure PVA was 4.510 [Å] shifted to 4.614 [Å] for PVA/ZnO/GCNF film. This shift resulted from hydrogen bonding interactions between these nanofillers and the PVA matrix [35]. Adding the fillers into PVA also led to an increase in peak intensity and a decrease in FWHM (full width at half-maximum) value indicating increased crystallinity index and crystal size (Table 2) [36]. The highest intensity diffraction peak was measured on PVA/ZnO/GCNF film, which indicated an enhancement of the crystal size of about 33% compared to pure PVA.

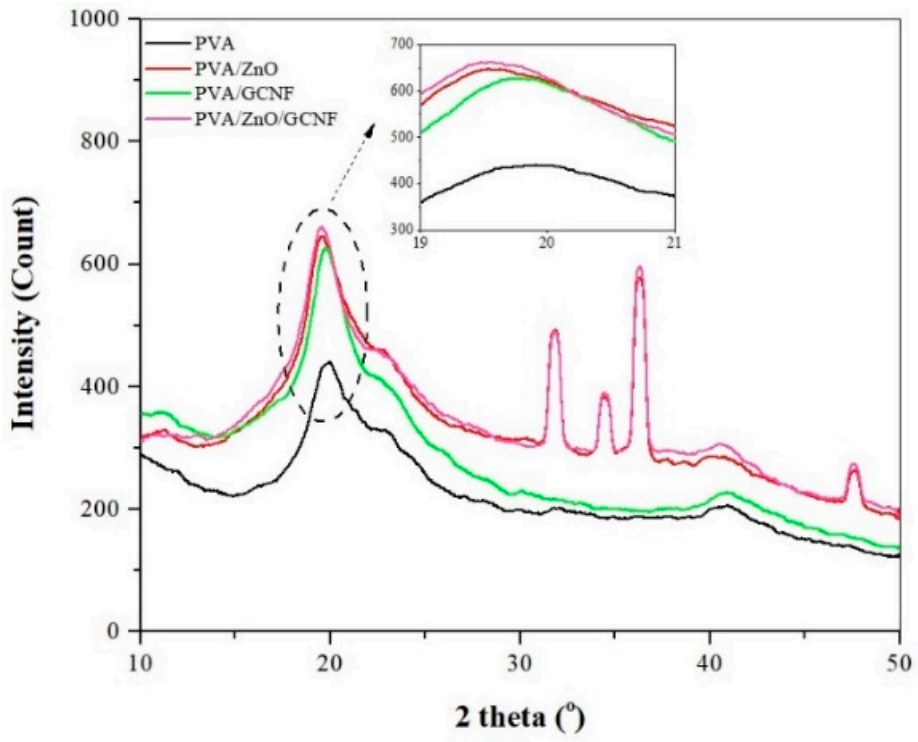

Figure 3. XRD pattern for samples.

Table 2. d-spacing, FWHM, and the peak position at 2θ around 19.6° of films recorded from X-ray diffraction testing from Figure 3, and T_m from Figure 4.

Samples	The Peak Position at 2θ around 19.6°	T_m (°C)	d-Spacing [Å] at 2θ (19.6°)	FWHM (°) of the Peak at 2θ (19.6°)
PVA	19.686	300	4.510	0.614
PVA/GCNF	19.667	301	4.514	0.614
PVA/ZnO	19.344	341	4.589	0.512
PVA/ZnO/GCNF	19.236	345	4.614	0.409

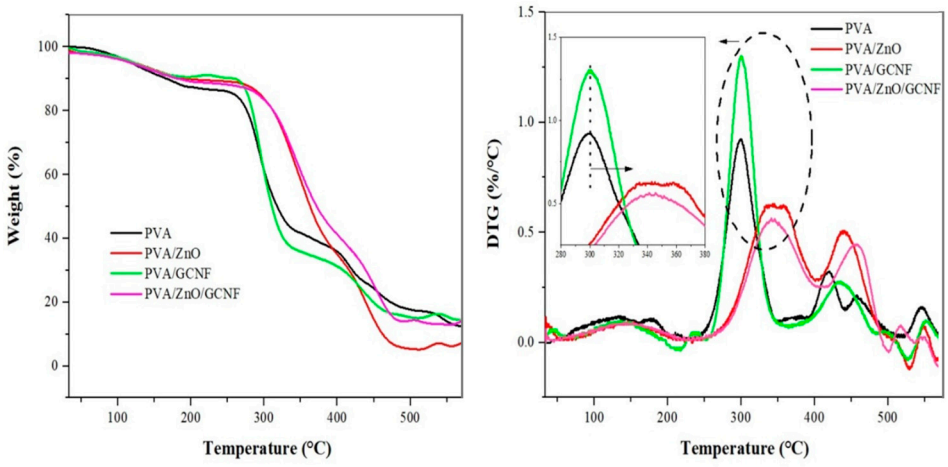

(a) **(b)**

Figure 4. TGA (**a**) and DTG (**b**) curve for all samples.

3.4. Thermal Analysis

Figure 4 shows the TGA (a) and DTG (b) curves of all tested films. Initially, the sample weight in the temperature range from 60 to 150 °C was slightly reduced due to absorbed water evaporation [37]. The films displayed different weight losses due to the different amounts of water available to evaporate. The PVA film had the highest evaporation corresponding to its highest hydrophilic nature and the highest number of free hydroxyl groups [8]. A sudden second weight loss (from 300 to 420 °C) occurs as a result of the decomposition of cellulose and the PVA matrix [31]. During this second weight-loss period, temperatures of the maximum rate of decomposition (T_m) of the films are presented in Table 2. The addition of nanofillers into the PVA matrix led to an increase in T_m, the thermal resistance of the film. The increased T_m relates to the increased fraction of nanofiller, which has higher thermal resistance than pure PVA [11]. The highest thermal resistance was measured on the PVA/ZnO/GCNF biocomposite film, which had T_m of 345 °C; 15% higher than T_m of pure PVA film. The high T_m of this film corresponds to an increased crystallinity index and crystal size from a decreased FWHM value (Table 2 and Figure 3). An increased crystalline structure leads to a higher resistance to heat and a higher thermal decomposition temperature [38]. This result agrees with previous research [39]. Strong interfacial hydrogen bonding between PVA and nanofillers dispersed homogeneously in the matrix also contributes to the thermal stability of the biocomposite films, consequently reducing the weight loss in the sample [40]. For further heating of the films over 420 °C, a third weight loss is detected due to the decomposition of ash [41].

3.5. Tensile Properties

Figure 5 displays tensile properties all films, including TS (Figure 5a), TM (Figure 5b), and EB (Figure 5c). Some of the PVA composite film's tensile strength for food packaging applications reported in the literature are shown in Table 3. Pure PVA film presents the lowest TS value (12.0 MPa) and TM (116.2 MPa), and a high EB of 65.3%. Adding ZnO and/or GCNF fillers to the PVA matrix increased TS and TM without decreasing EB significantly. The PVA/ZnO/GCNF biocomposite film had the highest TS (19.7 MPa) and TM (253.1 MPa), increasing around 63.9% and 117.9%, respectively, in comparison with pure PVA film. This increase is expected because ZnO and GCNF anchored the polymer chains of PVA against the movement. As previously stated, homogeneous beach marks on all fracture surfaces shown in the FESEM photograph (Figure 1c) indicate well-dispersed fillers in the PVA matrix. These filler surfaces formed intermolecular hydrogen bonds to the PVA matrix, as evidenced by the FTIR spectra (Figure 2). These anchoring bonds led to an increase in TS and TM of the film. This result agrees with our prior study [19]. Though tensile strength and modulus increased, EB (56.6%) did not decrease significantly with

added filler loadings. This phenomenon is because the relatively longer tortuous path of the crack propagates through a weaker section of the film.

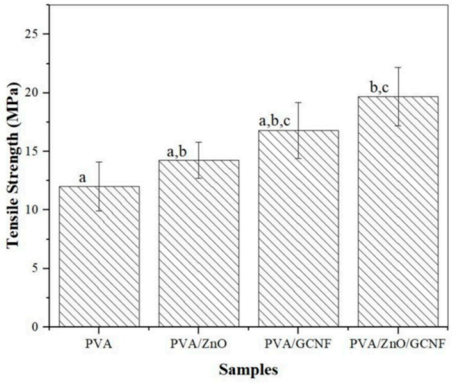

(**a**)

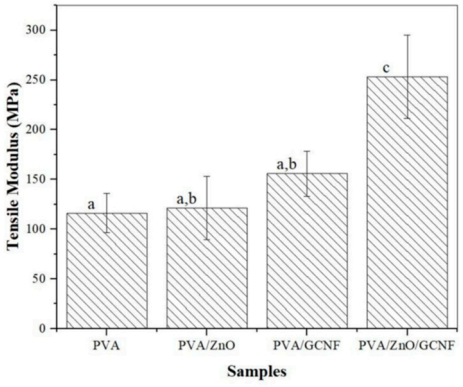

(**b**)

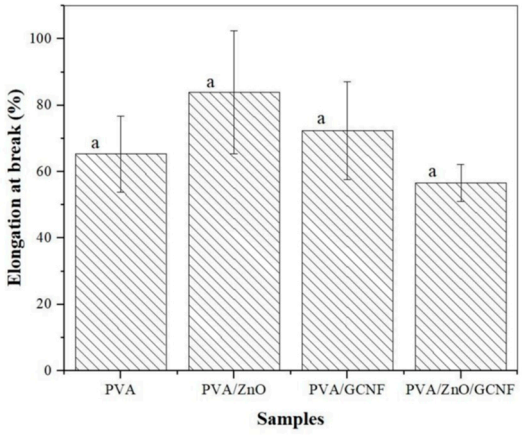

(**c**)

Figure 5. TS (**a**), TM (**b**), and EB (**c**) of each sample. Different letters (a–c) denote a significant difference in mean values ($p \leq 0.05$).

Table 3. The PVA composite film for food packaging applications reported in literature.

Author	Material	Tensile Strength (MPa)
Dieter et al. [This Work]	PVA/ZnO/GCNF	19.7
Abral et al. [33]	PVA/cassava starch	17.2
Sarwar et al. [37]	PVA/nanocellulose/Ag	12.32
Jayakumar et al. [42]	PVA/starch/nutmeg oil/ZnO/jamun extract	26
Mustafa et al. [43]	PVA/starch/propolis/anthocyanins rosemary extract	6
Bazzi et al. [44]	PVA/chitosan/graphene nanoplatelets	11
Yang et al. [45]	PVA/nanolignin	24.3
Amalraj et al. [46]	PVA/gum arabic/chitosan	11.8
Cano et al. [47]	PVA/neem oil	21.5
Francis et al. [48]	PVA/starch/glycerol	18.05

3.6. Antimicrobial Activity

One weakness of the currently available PVA is that it is easy to overgrow with the microbe. Figure 6 presents the antimicrobial activity of all samples against gram-negative bacteria, gram-positive bacteria, and fungi. The inhibition zone (in millimeters) and standard deviations were calculated and are presented in Table 4. This inhibition zone is indicating that the sample stops the bacteria from growing or kills the bacteria.

Table 4. Antimicrobial properties of each sample.

Samples	The Inhibition Zone Diameter with Standard Deviation (mm)				
	SA	BS	EC	PA	CA
PVA	0	0	0	0	0
PVA/ZnO	5.5 ± 0.04	5.3 ± 0.2	5.1 ± 0.7	4.7 ± 0.1	9.6 ± 1.5
PVA/GCNF	8.8 ± 1.8	12.4 ± 0.5	11.9 ± 1.7	12.0 ± 1.6	10.1 ± 1.0
PVA/ZnO/GCNF	13.6 ± 0.3	13.0 ± 0.5	14.5 ± 0.3	12.5 ± 0.9	11.2 ± 1.0
Positive Control	26.9 ± 0.2	25.6 ± 0.5	30.7 ± 0.4	26.5 ± 0.2	23.5 ± 0.5

It can be observed from the table that pure PVA does not have any antibacterial activity against microbes. A red arrow in Figure 6e confirms the fact that the microbes occupied the PVA sample. However, after adding the GCNF, the biocomposite shows a higher antimicrobial resistance signed with a transparent circle (blue arrow in Figure 6e) declaring the inhibition zone. This phenomenon is because the nano-materials disrupt bacterial cell membrane proteins resulting in the death of microbes [49]. White ginger contains a range of bioactive secondary metabolites like phenolic compounds, aldehydes, and ketones responsible for the broad antimicrobial spectrum [50]. Surprisingly, GCNF inhibited bacteria growth more strongly than ZnO because it contributed a higher concentration of bioactive compounds to the film. The PVA/GCNF biocomposite film displayed antifungal activity against *Candida Albicans*, as shown in previous work [51]. The most robust antimicrobial performance belongs to PVA/ZnO/GCNF biocomposite film (13 mm inhibition zone diameter average), attributable to the presence of both bioactive compounds (ZnO and GCNF fillers). Other published work stated that ZnO is biocompatible and safe for human and animal health [52,53]. These results indicate that the use of PVA/ZnO/GCNF film could be an eco-friendly, cost-effective food packaging to help preserve the freshness of food.

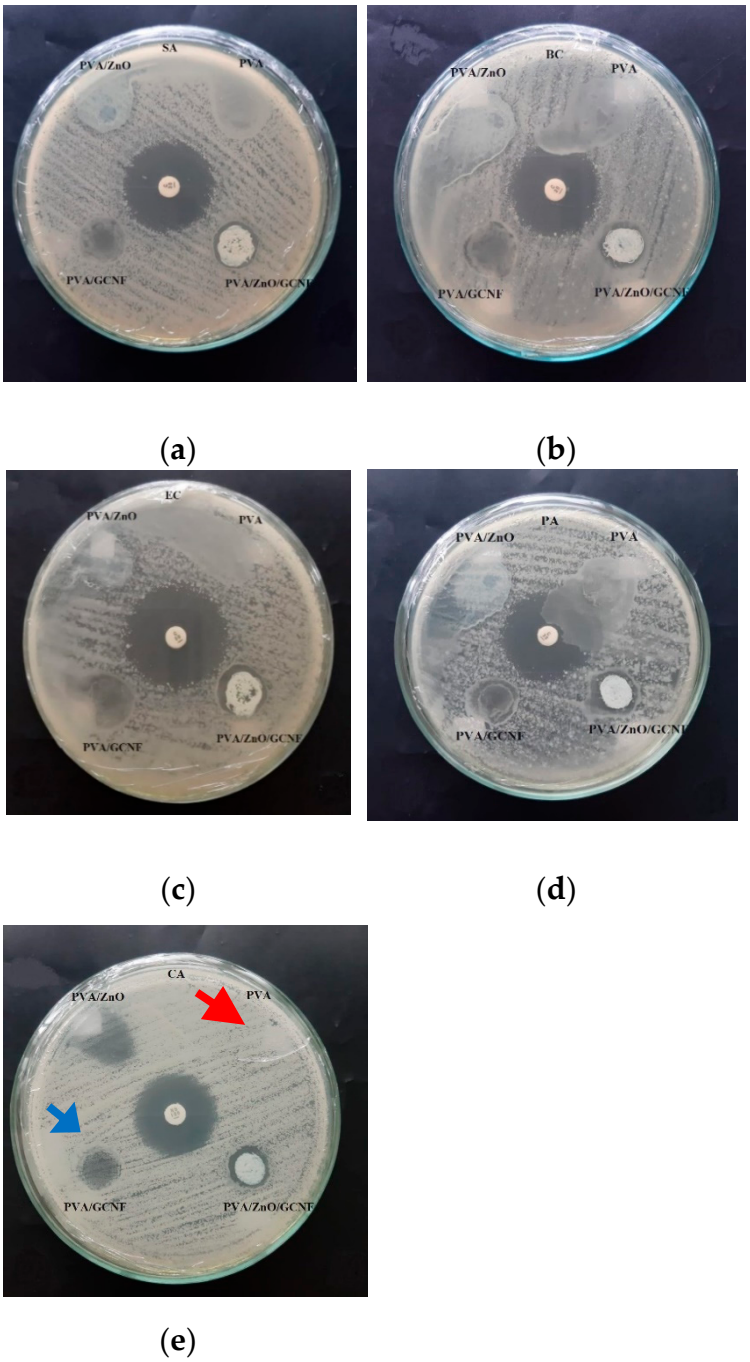

Figure 6. Antimicrobial activity of PVA and biocomposite film against gram-positive SA (**a**), BS (**b**), PA (**c**), EC (**d**), and CA (**e**). The more transparent area (blue and red arrows) is the inhibition zone diameter.

4. Conclusions

A PVA-based biocomposite film reinforced by ZnO nanoparticles and white ginger cellulose nanofiber from residue ginger fibers was successfully prepared for the first time. The PVA/ZnO/GCNF biocomposite film has demonstrated excellent performance with the highest value of TS (19.7 MPa), TM (253.1 MPa), thermal resistance (345 °C), and inhibition zone of antimicrobial activity(14.5 $\pm$ 0.3 mm). According to the antimicrobial test results, it can be seen that the addition of ZnO and GCNF increased the inhibition zone diameter, which indicated that it is more resistant to bacteria. It also increased the crystal size by about 33% compared with the pure PVA sample. However, despite increased TS and TM values, the PVA/ZnO/GCNF film still had a high EB value corresponding to high

formability. Therefore, the PVA/ZnO/GCNF-based film prepared in the study might offer a cheap potential material for food packaging.

Author Contributions: Conceptualization, H.A.; Data curation, W.H.Y., D.H., N.S., E.S., A.N.M., S.M.S. and R.A.I.; Formal analysis, D.H.; Funding acquisition, H.A.; Investigation, W.H.Y., N.S., E.S., A.N.M. and S.M.S.; Methodology, D.R.; Resources, A.N.M. and R.A.I.; Supervision, D.R.; Validation, D.R. and D.H.; Writing—review & editing, D.R. and H.A. All authors have read and agreed to the published version of the manuscript.

Funding: This research was funded by Universitas Andalas grant number T/7/UN.16.17/PT.01.03/PRK-PDU-KRP1GB-Unand/2022. The APC was funded by Universitas Andalas.

Data Availability Statement: The data presented in this study are available on request from the corresponding author.

Acknowledgments: Acknowledgment is addressed to Universitas Andalas for supporting research funding with project name Penelitian Dasar Unggulan Universitas Andalas Klaster Riset-Publikasi Bereputasi (PDU-KRP1GB-Unand), number T/7/UN.16.17/PT.01.03/PRK-PDU-KRP1GB-Unand/2022 and to Fakultas Teknik, Universitas Andalas (Padang, Indonesia) for assisting research funding 2021.

Conflicts of Interest: The authors declare no conflict of interest.

References

1. Maurya, M.; Maurya, N.K.; Bajpai, V. Effect of SiC Reinforced Particle Parameters in the Development of Aluminium Based Metal Matrix Composite. *Evergreen* **2019**, *6*, 200–206. [CrossRef]
2. Syahrial, A.Z.; Miqdad, M.; Syahrial, A.Z. Effect of Nano Al2O3 Addition and T6 Heat Treatment on Characteristics of AA7075 / Al_2O_3 Composite Fabricated by Squeeze Casting Method for Ballistic Application Effect of Nano Al_2O_3 Addition and T6 Heat Treatment on Characteristics of AA. *Evergreen* **2022**, *9*, 531–537.
3. Rahmadiawan, D.; Aslfattahi, N.; Nasruddin, N.; Saidur, R.; Arifutzzaman, A.; Mohammed, H.A. MXene Based Palm Oil Methyl Ester as an Effective Heat Transfer Fluid. *J. Nano Res.* **2021**, *68*, 17–34. [CrossRef]
4. Bhargava, N.; Sharanagat, V.S.; Mor, R.S.; Kumar, K. Active and Intelligent Biodegradable Packaging Films Using Food and Food Waste-Derived Bioactive Compounds: A Review. *Trends Food Sci. Technol.* **2020**, *105*, 385–401. [CrossRef]
5. Mathew, S.; Mathew, J.; Radhakrishnan, E.K. Polyvinyl Alcohol/Silver Nanocomposite Films Fabricated under the Influence of Solar Radiation as Effective Antimicrobial Food Packaging Material. *J. Polym. Res.* **2019**, *26*, 1–10. [CrossRef]
6. Agarwal, S.; Hoque, M.; Bandara, N.; Pal, K.; Sarkar, P. Synthesis and Characterization of Tamarind Kernel Powder-Based Antimicrobial Edible Films Loaded with Geraniol. *Food Packag. Shelf Life* **2020**, *26*, 100562. [CrossRef]
7. Oner, B.; Meral, R.; Ceylan, Z. Determination of Some Quality Indices of Rainbow Trout Fillets Treated with Nisin-Loaded Polyvinylalcohol-Based Nanofiber and Packed with Polyethylene Package. *Lwt* **2021**, *149*, 111854. [CrossRef]
8. Lee, H.; You, J.; Jin, H.J.; Kwak, H.W. Chemical and Physical Reinforcement Behavior of Dialdehyde Nanocellulose in PVA Composite Film: A Comparison of Nanofiber and Nanocrystal. *Carbohydr. Polym.* **2020**, *232*, 115771. [CrossRef] [PubMed]
9. Abral, H.; Atmajaya, A.; Mahardika, M.; Hafizulhaq, F.; Kadriadi; Handayani, D.; Sapuan, S.M.; Ilyas, R.A. Effect of Ultrasonication Duration of Polyvinyl Alcohol (PVA) Gel on Characterizations of PVA Film. *J. Mater. Res. Technol.* **2020**, *9*, 2477–2486. [CrossRef]
10. Abral, H.; Ikhsan, M.; Rahmadiawan, D.; Handayani, D.; Sandrawati, N.; Sugiarti, E.; Novi, A. Anti-UV, Antibacterial, Strong, and High Thermal Resistant Polyvinyl Alcohol/Uncaria Gambir Extract Biocomposite Film. *J. Mater. Res. Technol.* **2022**, *17*, 2193–2202. [CrossRef]
11. Darbasizadeh, B.; Fatahi, Y.; Feyzi-barnaji, B.; Arabi, M.; Motasadizadeh, H.; Farhadnejad, H.; Moraffah, F.; Rabiee, N. Crosslinked-Polyvinyl Alcohol-Carboxymethyl Cellulose/ZnO Nanocomposite Fibrous Mats Containing Erythromycin (PVA-CMC/ZnO-EM): Fabrication, Characterization and in-Vitro Release and Anti-Bacterial Properties. *Int. J. Biol. Macromol.* **2019**, *141*, 1137–1146. [CrossRef]
12. Zhu, Q.; Zhao, Y.; Miao, B.; Abo-Dief, H.M.; Qu, M.; Pashameah, R.A.; Xu, B.B.; Huang, M.; Algadi, H.; Liu, X.; et al. Hydrothermally Synthesized ZnO-RGO-PPy for Water-Borne Epoxy Nanocomposite Coating with Anticorrosive Reinforcement. *Prog. Org. Coatings* **2022**, *172*, 107153. [CrossRef]
13. Zhang, R.; Wang, Y.; Ma, D.; Ahmed, S.; Qin, W.; Liu, Y. Effects of Ultrasonication Duration and Graphene Oxide and Nano-Zinc Oxide Contents on the Properties of Polyvinyl Alcohol Nanocomposites. *Ultrason. Sonochem.* **2019**, *59*, 104731. [CrossRef] [PubMed]
14. Dyartanti, E.R.; Widiasa, I.N.; Purwanto, A.; Susanto, H. Nanocomposite Polymer Electrolytes in PVDF/ZnO Membranes Modified with PVP for Use in LiFePo4 Batteries. *Evergreen* **2018**, *5*, 19–25. [CrossRef]
15. Jacob, J.; Peter, G.; Thomas, S.; Haponiuk, J.T.; Gopi, S. Chitosan and Polyvinyl Alcohol Nanocomposites with Cellulose Nanofibers from Ginger Rhizomes and Its Antimicrobial Activities. *Int. J. Biol. Macromol.* **2019**, *129*, 370–376. [CrossRef] [PubMed]
16. Adhikari, B. *Nepal Ginger Profile 2016: An Assessment of Commercial Ginger Cultivated in Nepal*; Nepal Market Development Nepal & Ginger Producers and Traders: Kathmandu, Nepal, 2016.

17. Thomas, S.; Gopi, S.; Jacob, J.; Haponiuk, J.; Peter, G. Use of Ginger Nanofibers for the Preparation of Cellulose Nanocomposites and Their Antimicrobial Activities. *Fibers* **2018**, *6*, 79. [CrossRef]
18. Abral, H.; Ariksa, J.; Mahardika, M.; Handayani, D.; Aminah, I.; Sandrawati, N.; Pratama, A.B.; Fajri, N.; Sapuan, S.M.; Ilyas, R.A. Transparent and Antimicrobial Cellulose FIlm from Ginger Nanofiber. *Food Hydrocoll.* **2020**, *98*, 105266. [CrossRef]
19. Abral, H.; Ariksa, J.; Mahardika, M.; Handayani, D.; Aminah, I.; Sandrawati, N.; Sapuan, S.M.; Ilyas, R.A. Highly Transparent and Antimicrobial PVA Based Bionanocomposites Reinforced by Ginger Nanofiber. *Polym. Test.* **2019**, *81*, 106186. [CrossRef]
20. Abral, H.; Kurniawan, A.; Rahmadiawan, D.; Handayani, D.; Sugiarti, E.; Muslimin, A.N. Highly Antimicrobial and Strong Cellulose-Based Biocomposite Film Prepared with Bacterial Cellulose Powders, Uncaria Gambir, and Ultrasonication Treatment. *Int. J. Biol. Macromol.* **2022**, *208*, 88–96. [CrossRef] [PubMed]
21. Ariawan, D.; Raharjo, W.P.; Diharjo, K.; Raharjo, W.W.; Kusharjanta, B. Influence of Tropical Climate Exposure on the Mechanical Properties of RHDPE Composites Reinforced by Zalacca Midrib Fibers. *Evergreen* **2022**, *09*, 662–672.
22. Sosiati, H.; Yuniar, N.D.M.; Saputra, D.; Hamdan, S. The Influence of Carbon Fiber Content on the Tensile, Flexural, and Thermal Properties of the Sisal/PMMA Composites. *Evergreen* **2022**, *9*, 32–40. [CrossRef]
23. Rahmadiawan, D.; Abral, H.; Nasruddin, N.; Fuadi, Z. Stability, Viscosity, and Tribology Properties of Polyol Ester Oil-Based Biolubricant Filled with TEMPO-Oxidized Bacterial Cellulose Nanofiber. *Int. J. Polym. Sci.* **2021**, *2021*, 5536047. [CrossRef]
24. Fuadi, Z.; Rahmadiawan, D.; Kurniawan, R.; Mulana, F.; Abral, H. Effect of Graphene Nanoplatelets on Tribological Properties of Bacterial Cellulose/Polyolester Oil Bio-Lubricant. *Front. Mech. Eng.* **2022**, *8*, 810847. [CrossRef]
25. Abral, H.; Pratama, A.B.; Handayani, D.; Mahardika, M.; Aminah, I.; Sandrawati, N.; Sugiarti, E.; Muslimin, A.N.; Sapuan, S.M.; Ilyas, R.A. Antimicrobial Edible Film Prepared from Bacterial Cellulose Nanofibers/Starch/Chitosan for a Food Packaging Alternative. *Int. J. Polym. Sci.* **2021**, *2021*, 6641284. [CrossRef]
26. Bauer, A.W.; Kirby, W.M.M.; Sherris, J.C.; Turck, M. Antibiotic Susceptibility Testing by a Standardized Single Disk Method. *Am. J. Clin. Pathol.* **1966**, *36*, 493–496. [CrossRef]
27. Chen, C.; Ding, R.; Yang, S.; Wang, J.; Chen, W.; Zong, L.; Xie, J. Development of Thermal Insulation Packaging Film Based on Poly(Vinyl Alcohol) Incorporated with Silica Aerogel for Food Packaging Application. *Lwt* **2020**, *129*, 109568. [CrossRef]
28. Abral, H.; Soni Satria, R.; Mahardika, M.; Hafizulhaq, F.; Affi, J.; Asrofi, M.; Handayani, D.; Sapuan, S.M.; Stephane, I.; Sugiarti, E.; et al. Comparative Study of the Physical and Tensile Properties of Jicama (Pachyrhizus Erosus) Starch Film Prepared Using Three Different Methods. *Starch/Staerke* **2019**, *71*, 1–9. [CrossRef]
29. Hezma, A.M.; Rajeh, A.; Mannaa, M.A. An Insight into the Effect of Zinc Oxide Nanoparticles on the Structural, Thermal, Mechanical Properties and Antimicrobial Activity of Cs/PVA Composite. *Colloids Surfaces A Physicochem. Eng. Asp.* **2019**, *581*, 123821. [CrossRef]
30. Mahardika, M.; Abral, H.; Kasim, A.; Arief, S.; Hafizulhaq, F.; Asrofi, M. Properties of Cellulose Nanofiber/Bengkoang Starch Bionanocomposites: Effect of Fiber Loading. *LWT Food Sci. Technol.* **2019**, *116*, 108554. [CrossRef]
31. Abral, H.; Fajri, N.; Mahardika, M.; Handayani, D.; Sugiarti, E.; Kimd, H.J. A Simple Strategy in Enhancing Moisture and Thermal Resistance and Tensile Properties of Disintegrated Bacterial Cellulose Nanopaper. *J. Mater. Res. Technol.* **2020**, *9*, 8754–8765. [CrossRef]
32. Channa, I.A.; Ashfaq, J.; Gilani, S.J.; Shah, A.A.; Chandio, A.D.; Jumah, M.N. Bin UV Blocking and Oxygen Barrier Coatings Based on Polyvinyl Alcohol and Zinc Oxide Nanoparticles for Packaging Applications. *Coatings* **2022**, *12*, 897. [CrossRef]
33. Abral, H.; Hartono, A.; Hafizulhaq, F.; Handayani, D.; Sugiarti, E.; Pradipta, O. Characterization of PVA/Cassava Starch Biocomposites Fabricated with and without Sonication Using Bacterial Cellulose Fiber Loadings. *Carbohydr. Polym.* **2018**, *206*, 593–601. [CrossRef] [PubMed]
34. Khalid, A.; Khan, R.; Ul-Islam, M.; Khan, T.; Wahid, F. Bacterial Cellulose-Zinc Oxide Nanocomposites as a Novel Dressing System for Burn Wounds. *Carbohydr. Polym.* **2017**, *164*, 214–221. [CrossRef] [PubMed]
35. Patil, S.L.; Pawar, S.G.; Chougule, M.A.; Raut, B.T.; Godse, P.R.; Sen, S.; Patil, V.B. Structural, Morphological, Optical, and Electrical Properties of PANi-ZnO Nanocomposites. *Int. J. Polym. Mater.* **2012**, *61*, 809–820. [CrossRef]
36. Ul-Islam, M.; Khattak, W.A.; Ullah, M.W.; Khan, S.; Park, J.K. Synthesis of Regenerated Bacterial Cellulose-Zinc Oxide Nanocomposite Films for Biomedical Applications. *Cellulose* **2014**, *21*, 433–447. [CrossRef]
37. Sarwar, M.S.; Niazi, M.B.K.; Jahan, Z.; Ahmad, T.; Hussain, A. Preparation and Characterization of PVA/Nanocellulose/Ag Nanocomposite Films for Antimicrobial Food Packaging. *Carbohydr. Polym.* **2018**, *184*, 453–464. [CrossRef]
38. Abral, H.; Dalimunthe, M.H.; Hartono, J.; Efendi, R.P.; Asrofi, M.; Sugiarti, E.; Sapuan, S.; Park, J.-W.; Kim, H.-J. Characterization of Tapioca Starch Biopolymer Composites Reinforced with Micro Scale Water Hyacinth Fibers. *Starch Stärke* **2018**, *70*, 1700287. [CrossRef]
39. Asrofi, M.; Abral, H.; Kurnia, Y.; Sapuan, S.M.; Kim, H. Effect of Duration of Sonication during Gelatinization on Properties of Tapioca Starch Water Hyacinth Fiber Biocomposite. *Int. J. Biol. Macromol.* **2018**, *108*, 167–176. [CrossRef]
40. Asrofi, M.; Abral, H.; Kasim, A.; Pratoto, A.; Mahardika, M.; Hafizulhaq, F. Characterization of the Sonicated Yam Bean Starch Bionanocomposites Reinforced By Nanocellulose Water Hyacinth Fiber (Whf): The Effect of Various Fiber Loading. *J. Eng. Sci. Technol.* **2018**, *13*, 2700–2715.
41. Syafri, E.; Kasim, A.; Abral, H.; Asben, A. Cellulose Nanofibers Isolation and Characterization from Ramie Using a Chemical-Ultrasonic Treatment. *J. Nat. Fibers* **2019**, *16*, 1145–1155. [CrossRef]

42. Jayakumar, A.; Heera, K.V.; Sumi, T.S.; Joseph, M.; Mathew, S.; Praveen, G.; Nair, I.C.; Radhakrishnan, E.K. Starch-PVA Composite Films with Zinc-Oxide Nanoparticles and Phytochemicals as Intelligent PH Sensing Wraps for Food Packaging Application. *Int. J. Biol. Macromol.* **2019**, *136*, 395–403. [CrossRef] [PubMed]
43. Mustafa, P.; Niazi, M.B.K.; Jahan, Z.; Samin, G.; Hussain, A.; Ahmed, T.; Naqvi, S.R. PVA/Starch/Propolis/Anthocyanins Rosemary Extract Composite Films as Active and Intelligent Food Packaging Materials. *J. Food Saf.* **2020**, *40*, e12725. [CrossRef]
44. Bazzi, M.; Shabani, I.; Mohandesi, J.A. Enhanced Mechanical Properties and Electrical Conductivity of Chitosan/Polyvinyl Alcohol Electrospun Nanofibers by Incorporation of Graphene Nanoplatelets. *J. Mech. Behav. Biomed. Mater.* **2022**, *125*, 104975. [CrossRef] [PubMed]
45. Yang, W.; Ding, H.; Qi, G.; Li, C.; Xu, P.; Zheng, T.; Zhu, X.; Kenny, J.M.; Puglia, D.; Ma, P. Highly Transparent PVA/Nanolignin Composite Films with Excellent UV Shielding, Antibacterial and Antioxidant Performance. *React. Funct. Polym.* **2021**, *162*, 104873. [CrossRef]
46. Amalraj, A.; Haponiuk, J.T.; Thomas, S.; Gopi, S. Preparation, Characterization and Antimicrobial Activity of Polyvinyl Alcohol/Gum Arabic/Chitosan Composite Films Incorporated with Black Pepper Essential Oil and Ginger Essential Oil. *Int. J. Biol. Macromol.* **2020**, *151*, 366–375. [CrossRef]
47. Cano, A.; Cháfer, M.; Chiralt, A.; González-Martínez, C. Physical and Antimicrobial Properties of Starch-Pva Blend Films as Affected by the Incorporation of Natural Antimicrobial Agents. *Foods* **2016**, *5*, 3. [CrossRef]
48. Francis, D.V.; Thaliyakattil, S.; Cherian, L.; Sood, N.; Gokhale, T. Metallic Nanoparticle Integrated Ternary Polymer Blend of PVA/Starch/Glycerol: A Promising Antimicrobial Food Packaging Material. *Polymers* **2022**, *14*, 1379. [CrossRef]
49. Raghupathi, K.R.; Koodali, R.T.; Manna, A.C. Size-Dependent Bacterial Growth Inhibition and Mechanism of Antibacterial Activity of Zinc Oxide Nanoparticles. *Langmuir* **2011**, *27*, 4020–4028. [CrossRef]
50. Beristain-Bauza, S.D.C.; Hernández-Carranza, P.; Cid-Pérez, T.S.; Ávila-Sosa, R.; Ruiz-López, I.I.; Ochoa-Velasco, C.E. Antimicrobial Activity of Ginger (Zingiber Officinale) and Its Application in Food Products. *Food Rev. Int.* **2019**, *35*, 407–426. [CrossRef]
51. Rinanda, T.; Isnanda, R.P. Zulfitri Chemical Analysis of Red Ginger (Zingiber Officinale Roscoe Var Rubrum) Essential Oil and Its Anti-Biofilm Activity against Candida Albicans. *Nat. Prod. Commun.* **2018**, *13*, 1587–1590. [CrossRef]
52. Xu, J.; Zhang, Y.; Gutha, Y.; Zhang, W. Antibacterial Property and Biocompatibility of Chitosan/Poly(Vinyl Alcohol)/ZnO (CS/PVA/ZnO) Beads as an Efficient Adsorbent for Cu(II) Removal from Aqueous Solution. *Colloids Surfaces B Biointerfaces* **2017**, *156*, 340–348. [CrossRef] [PubMed]
53. Swaroop, K.; Somashekarappa, H.M. In Vitro Biocompatibility and Antibacterial Activity of Gamma Ray Crosslinked ZnO/PVA Hydrogel Nanocomposites. *Mater. Today Proc.* **2018**, *5*, 21314–21321. [CrossRef]